

## **Effect of the Surface Structure of Gold Electrodes on the Coadsorption of Water and Anions**

Nuria Garcia-Araez<sup>\*1,2,3</sup>, Paramaconi Rodriguez<sup>2,3</sup>, Huib J. Bakker<sup>1</sup>, Marc T.M. Koper<sup>2</sup>

<sup>1</sup>FOM Institute for Atomic and Molecular Physics (AMOLF), Postbus 41883, 1009 DB Amsterdam, The Netherlands

<sup>2</sup>Leiden Institute of Chemistry, Leiden University, Postbus 9502, 2300 RA Leiden, The Netherlands

<sup>3</sup> Electrochemistry Laboratory, Paul Scherrer Institut, CH-5232 Villigen PSI, Switzerland (present address)

\* Corresponding author: Tel. +41 56 310 5737. E-mail: nuria.garcia-araez@psi.ch

## Abstract

The potential-dependent water adsorption on gold surfaces in perchloric and sulfuric acid solutions has been studied by surface-enhanced infrared absorption spectroscopy (SEIRAS). It is found that the surface structure of the gold electrodes has a major impact on the SEIRAS spectra. When the gold films are composed of nanoparticles of  $47 \pm 11$  nm, the SEIRAS spectra are in agreement with previous reports. However, when the size of the gold nanoparticles is decreased to  $27 \pm 8$  nm, by depositing the gold at  $1 \text{ \AA} / \text{s}$  instead of  $0.1 \text{ \AA} / \text{s}$ , it is found that the SEIRAS bands associated with water molecules coordinated to co-adsorbed anions are absent. The combination of both types of gold electrodes allows a detailed study of the properties of the adsorbed water molecules. It is found that water molecules coadsorbed with sulfate and perchlorate anions appear to belong to the hydration shell of the anions, because i) the intensity of the SEIRAS bands of these water molecules increase with potential in the same way as the SEIRAS bands of the adsorbed anions, and ii) the frequencies of the O-H stretch resemble those of the water molecules in the hydration shell of the anions in solution.

## 1. Introduction

The interaction of water with metal surfaces plays a central role in many disciplines such as catalysis, electrochemistry, and biochemistry. Being the most commonly used solvent, water can have a major impact on the rate and selectivity of reactions. For example, water has a promoting effect in the oxidation of CO and small alcohols on metal surfaces.<sup>1,2</sup> Water has also an important impact on the catalysis of the oxygen reduction reaction (ORR): water accelerates the oxidation of the metal in the presence of dissolved O<sub>2</sub>, and this has a detrimental effect on the rate of the ORR, since the catalysis of the ORR only takes place on the metallic surface.<sup>3-5</sup> As a result, gold is potentially a better catalyst than platinum for the ORR, due to its higher oxidation potential. Indeed, deposition of gold nanoparticles on platinum has shown to improve the stability of the catalyst for the ORR.<sup>6</sup> In conclusion, understanding the properties of interfacial water molecules and its interaction with coadsorbed ions is crucial to improve the catalytic performance of metal surfaces.

One of the main difficulties in the study of interfacial water is the interference from bulk water contributions. For this reason, most of the progress in the understanding of the interaction of water with metal surfaces has arisen from model experiments under ultra-high-vacuum (UHV) conditions and theoretical works.<sup>7-14</sup> Surface-Enhanced Raman Scattering (SERS) has also been successfully applied for the study of water adsorption on metal electrodes under electrochemical conditions.<sup>15-18</sup> SERS is suitable to study, for example, the effect of the composition of the metal electrode and the applied electrochemical potential. However, SERS measurements require rough electrodes, and it is believed that the signal originates from hot spots with peculiar geometries. Therefore, this technique is not adequate to characterize the effect of the surface structure of the electrode. Sum-Frequency Generation (SFG) has also been used to study water adsorption on metals under electrochemical conditions,<sup>19-21</sup> but it should be noted that the interpretation of SFG spectra is far from being straight-forward. Finally, the potential-dependent adsorption of water on metal electrodes has also been studied by the laser-induced temperature jump method<sup>22,23</sup> and contact angle measurements.<sup>24</sup> These techniques have been used to determine the reorientation of water molecules on metals,

but they do not provide any chemical information about the properties of interfacial water.

One technique that is especially well suited to study the properties of water molecules is infrared spectroscopy. The characteristic infrared adsorption bands of water molecules provide a wealth of information about the interaction with the environment, hydrogen-bonding strength, conformation, mobility, etc.<sup>25-27</sup> In order to study the infrared spectrum of interfacial water at electrochemical interfaces, it is advantageous to perform the measurements under conditions of attenuated total reflection. In these experiments, the electrode is a thin metal film deposited on a highly-refractive, transparent prism. The infrared beam passes through the prism and is totally reflected at the metal-prism interface with an evanescent wave penetrating into the metal-solution interface, thereby probing the absorption of interfacial species. Under certain conditions, enhancement of the absorption signal of interfacial species takes place (SEIRAS: Surface-Enhanced Infrared Absorption Spectroscopy). As a result, the measured signal is dominated by the response of interfacial species, and the contributions from bulk species can be subtracted by calculating the difference of the measured response at different potentials. This methodology has been successfully applied to the study of interfacial water on gold thin films in several works.<sup>28-44</sup>

In a recent paper,<sup>45</sup> we showed that the SEIRAS spectra of water on gold in sulfuric acid solutions were markedly dependent on the preparation method of the gold electrode. When the gold thin film was deposited on the silicon substrate with a deposition rate of 1 Å/s, the water molecules coadsorbed with sulfate anions became effectively invisible in the SEIRAS spectra. AFM images demonstrated that these gold films were composed of small nanoparticles of  $27 \pm 8$  nm. In the present work, we extend this study to perchloric acid solutions. The comparison with previous results obtained in sulfuric acid solutions allows a unique understanding of the properties of interfacial water molecules coadsorbed with different anions. The selection of sulfate and perchlorate anions for this comparison is due to the very different hydration properties of these anions.<sup>25,26,46</sup> Sulfate anions form strong hydrogen bonds with water molecules, with a local structure similar to the pure water hydrogen bond network. Consequently, the vibrational properties of water molecules in the hydration shell of sulfate anions are

similar to bulk water (the O-H stretch frequency is nearly the same). On the contrary, water molecules bonding to perchlorate anions behave quite differently from bulk water. The strength of the hydrogen bonds formed between water molecules and perchlorate anions is much smaller than in the case of sulfate anions. The number of hydrogen bonds per water molecule in the hydration shell of perchlorate anions is quite small, and consequently, the O-H stretch adsorption band is significantly narrower and blue shifted with respect to bulk water.<sup>25,26</sup>

## 2. Experimental Methods

The SEIRAS experiments were carried out with a Bruker Vertex80V vacuum FTIR spectrometer, equipped with a liquid-nitrogen cooled Hg-Cd-Te detector, employing the Krestchmann ATR configuration. The spectrometer operates at a pressure <1.8 hPa, so that interference due to the absorption of water vapors or CO<sub>2</sub> in the optical path is virtually eliminated. Leaking of the electrolyte solution towards the optical bench is avoided with the use of Teflon O-rings. The spectra were collected with p-polarized light with a resolution of 6 cm<sup>-1</sup>. The incident angle was 60° from the surface normal. 16 interferograms were averaged for each spectrum, resulting in an acquisition time of 5 seconds per spectrum. During the experiments, the potential was scanned at 20 mV/s, and thus, each spectrum represents the average IR response of a potential interval of 100 mV. All spectra are presented as  $\log(R_0/R_1)$ , where  $R_1$  and  $R_0$  represent the intensities of the reflected beam at the sample and reference potentials, respectively. Positive adsorption bands correspond to species more strongly adsorbed at the sample potential, while negative adsorption bands are due to species more strongly adsorbed at the reference potential.

The gold thin layers were deposited on a silicon prism by using electron beam evaporation in a UHV system (pressure <2x10<sup>-6</sup> mbar). The evaporation rate and the final gold thickness were controlled with a quartz crystal microbalance. Prior to the experiments, the thin gold deposit was cleaned with acetone, isopropanol and thorough rinsing with ultra-pure water. The cell and all glassware were immersed overnight in a concentrated solution of KMnO<sub>4</sub> that was slightly acidic. Later the solution was removed

and the residual  $\text{MnO}_4^-$  was treated with a diluted solution of  $\text{H}_2\text{O}_2$  and sulfuric acid (3:1) and finally thoroughly washed with ultra-pure water.

The electrochemical measurements were performed with an Autolab PGSTAT12. A gold wire was used as the counter electrode and a reversible hydrogen electrode (RHE) as the reference electrode. All potentials in this work are referred to the RHE scale. The electrical contact with the thin gold deposit was achieved with the help of a thin gold foil, which was not in contact with the solutions. Solutions were prepared from high purity reagents ( $\text{HClO}_4$  from Merck Suprapur) and ultra-pure water (Millipore MilliQ gradient A10 system,  $18.2 \text{ M}\Omega \text{ cm}$ ,  $<5 \text{ ppb}$  total organic carbon). Ar (N66) was used to deoxygenate all solutions. For the voltammogram presented here, the normalization of current to current density has been performed by using the geometrical area of the gold film in contact with the solutions ( $0.785 \text{ cm}^2$ ).

### 3. Results and discussion

#### 3.1. Cyclic voltammograms

Figure 1 shows a typical cyclic voltammogram of a thin gold film in  $0.1 \text{ M HClO}_4$ . This characteristic voltammogram indicates that the gold film is clean and exhibits domains with Au(111) orientation.<sup>47,48</sup> We measured essentially the same voltammogram for all gold films with thicknesses ranging from 20 to 30 nm, and with gold deposition rates varying between  $0.1\text{-}1 \text{ \AA/s}$ .

#### 3.1. SEIRAS measurements in perchloric acid solutions

Figures 2 and 3 show a series of typical SEIRAS spectra measured in an aqueous solution of  $0.1 \text{ M HClO}_4$  with gold films prepared at two different deposition rates, namely,  $0.1$  and  $1 \text{ \AA/s}$ , respectively. For all films with a thickness varying between 20 and 30 nm, essentially the same results were obtained. While the SEIRAS spectra in Figure 2 are in good agreement with a previous publication by Osawa and coworkers,<sup>28</sup> the results in Figure 3, obtained with a faster deposition rate, are markedly different. In a recent publication,<sup>45</sup> we reported a similar effect of the deposition rate on the SEIRAS spectra measured in an aqueous solution of  $0.1 \text{ M H}_2\text{SO}_4$ . Here we demonstrate that this effect is not specific to sulfuric acid solutions.

We will follow the work by Osawa and coworkers<sup>28</sup> for the assignment of the SEIRAS bands in Figure 2. It should be recalled that all the spectra reported are potential difference spectra measured with respect to a reference spectrum at  $E_{\text{ref}}=0.05$  V. At such a low reference potential, the amount of anion adsorption is negligible. Consequently, the SEIRAS bands in Figure 2 can be assigned as follows:

-The positive band at  $1050\text{-}1150\text{ cm}^{-1}$ , whose magnitude increases monotonically with potential from  $E>0.4$  V, is associated with the Cl-O stretching mode,  $\nu(\text{Cl-O})$ , of adsorbed perchlorate.

-Interfering with the  $\nu(\text{Cl-O})$  perchlorate band, there is a small negative band at  $1115\text{ cm}^{-1}$ , which is due to the Si-O stretching of silicon oxide. This band appears because the gold deposits are formed by islands or grains, and in between these islands, some patches of the silicon surface are exposed to the aqueous solution, producing the slow growth of a silicon oxide layer.<sup>45</sup>

-At  $E\leq 0.4$  V, there is a negative band near  $3470\text{ cm}^{-1}$  associated with the O-H stretch mode,  $\nu(\text{O-H})$ , of interfacial water, and a negative band at  $1615\text{ cm}^{-1}$ , associated with the H-O-H bending mode,  $\delta(\text{H-O-H})$ . These signatures have been ascribed to water molecules adsorbed with their hydrogen atoms somewhat closer to the gold surface (see Figure 4A).<sup>28</sup> In this orientation, the oxygen lone-pair orbital interacts with the gold surface, explaining the observed low frequency of the  $\delta(\text{H-O-H})$  mode (compared to bulk water). In addition, formation of hydrogen bonds with other water molecules would be hindered in this orientation, in agreement with the observed high frequency of the  $\nu(\text{O-H})$  mode. On the other than, in this orientation, the molecular axis is inclined by about  $109^\circ$  from the surface normal, which would suggest that, in principle, the magnitude of the  $\nu(\text{O-H})$  and  $\delta(\text{H-O-H})$  bands would be small. However, there are other factors that affect the magnitude of infrared absorption bands, like the surface coverage and the derivative of the transition dipole moment with the reaction coordinate. This orientation is in agreement with theoretical studies on a negatively charged Au(111) surface.<sup>49</sup> However, model DFT calculations suggest water adsorption with one O-H bond pointing towards the surface,<sup>50</sup> or directed parallel to the surface.<sup>51</sup>

-At  $E\leq 0.4$  V, there is also a broad negative band near  $1700\text{ cm}^{-1}$ , which has been ascribed to the bending mode of the adsorbed hydronium cation. The actual species corresponding

to this band is probably not the  $\text{H}_3\text{O}^+$  cation, but other hydronium-water complexes like  $\text{H}_5\text{O}_2^+$ ,  $\text{H}_7\text{O}_3^+$  and  $\text{H}_9\text{O}_4^+$ .<sup>52,53</sup>

-At  $E \geq 0.5$  V, a broad positive  $\nu(\text{O-H})$  band near  $3200 \text{ cm}^{-1}$  starts to grow. This signature has been ascribed to water molecules adsorbed on gold in an ice-like structure (see Figure 4B). DFT model calculations have shown that this is the most favorable structure of a water bilayer on Au(111)<sup>54</sup> and Au nanoparticles.<sup>55</sup>

-Additionally, at  $E \geq 0.5$  V, a few other positive bands appear: a narrow  $\nu(\text{O-H})$  band at  $3610 \text{ cm}^{-1}$ , a  $\nu(\text{O-H})$  band near  $3400 \text{ cm}^{-1}$  and a  $\delta(\text{H-O-H})$  band at  $1650 \text{ cm}^{-1}$ . However, these bands overlap with the negative bands mentioned above, which are still present in the spectra. Indeed, the  $\nu(\text{O-H})$  band near  $3400 \text{ cm}^{-1}$  is partially hidden due to the overlapping with the negative  $\nu(\text{O-H})$  band at  $3470 \text{ cm}^{-1}$ , but further proof of the presence of this band will be given below. These new features have been ascribed to water molecules that are asymmetrically hydrogen bonded, i.e., water molecules with a non-hydrogen bonded O-H moiety (yielding the narrow  $\nu(\text{O-H})$  band at  $3610 \text{ cm}^{-1}$ ) and a hydrogen bonded O-H moiety (yielding the  $\nu(\text{O-H})$  band near  $3400 \text{ cm}^{-1}$ ). These water molecules are coordinating coadsorbed perchlorate anions, and their two most likely orientations are sketched in Figure 4C,D. These orientations are in agreement with theoretical studies on a positively charged Au(111) surface.<sup>49</sup> In these sketches, it is assumed that water molecules coordinate the perchlorate anions through the edges of the tetrahedron, as it is found in aqueous solutions.<sup>56,57</sup>

Next, we discuss the assignment of the spectra in Figure 3. Comparison with the spectra in Figure 2 shows that:

- The  $\nu(\text{Cl-O})$  band of adsorbed perchlorate is affected only marginally by the change in the gold deposition rate from  $0.1$  to  $1 \text{ \AA/s}$ . The only difference is that, at  $E \geq 0.9$  V, the frequency of the  $\nu(\text{Cl-O})$  band is somewhat higher with gold films made at  $1 \text{ \AA/s}$  (ca.  $1150 \text{ cm}^{-1}$ , vs. ca.  $1120 \text{ cm}^{-1}$  with gold films deposited at  $0.1 \text{ \AA/s}$ ).
- The signatures characteristic of interfacial water in the spectra at  $E \leq 0.4$  V remain also unaffected by the change in the gold deposition rate. Thus, it is concluded that the adsorption of water molecules with their hydrogen atoms closer to the gold (Figure 4A)

and the adsorption of the hydronium-water complexes are not affected by the gold deposition rate.

-The positive  $\nu(\text{O-H})$  band near  $3200\text{ cm}^{-1}$  is also present at  $E \geq 0.5\text{ V}$  in the spectra in Figure 3, evidencing that the adsorption of water in an ice-like structure (Figure 4B) is also unaffected by the gold deposition rate.

-Finally, at  $E \geq 0.5\text{ V}$ , the following positive bands are absent in the spectra in Figure 3: the narrow  $\nu(\text{O-H})$  band at  $3610\text{ cm}^{-1}$ , the  $\nu(\text{O-H})$  band near  $3400\text{ cm}^{-1}$  and the  $\delta(\text{H-O-H})$  band at  $1650\text{ cm}^{-1}$ . This means that the asymmetrically hydrogen bonded water molecules coordinating coadsorbed perchlorate anions (Figure 4C,D) become invisible when the gold deposition rate is changed from  $0.1$  to  $1\text{ \AA/s}$ .

Similar findings were obtained in our previous study of the effect of the gold deposition rate on the SEIRAS spectra in sulfuric acid.<sup>45</sup> We found that water molecules coordinating coadsorbed sulfate anions also became invisible when the gold deposition rate was increased from  $0.1$  to  $1\text{ \AA/s}$ . AFM images showed that gold films deposited at  $0.1\text{ \AA/s}$  are mainly composed of nanoparticles of  $47 \pm 11\text{ nm}$ , while gold films made at  $1\text{ \AA/s}$  are mainly formed by nanoparticles of  $27 \pm 8\text{ nm}$ . Noteworthy, the nanoparticle size affects the special range of the SEIRAS effect, in such a way that, with smaller nanoparticles, only species located in very close proximity to the surface are detected.<sup>58</sup> This is because the enhancement of the electric field at the interface associated to the excitation of surface plasmons decays steeply with the distance from the surface. SEIRAS signals of interfacial species will be proportional to  $(a + d)^{-10}$ , where  $a$  is the local radius of curvature of the nanoparticle and  $d$  is the distance from the surface.<sup>59,60</sup> Therefore, decreasing the nanoparticle size produces a more steeply decay of the SEIRAS intensity with the distance from the surface.

Consequently, it can be proposed that water molecules coadsorbed with sulfate and perchlorate anions are located at a certain distance from the surface. This would explain the fact that they are not detected in SEIRAS measurements with small nanoparticles. Alternatively, it can also be proposed that these water molecules are oriented flat on small gold nanoparticles. The size of the Au(111) domains will be smaller on smaller nanoparticles, and as a result, the adsorption of sulfate and perchlorate anions would be more disordered.<sup>61</sup> This could weaken the interaction with the

coadsorbed water molecules, leading to water adsorption near parallel to the surface, as predicted by DFT model calculations of water monomers on Au(111).<sup>54,62</sup> Finally, it should be noted that the SEIRAS spectra presented here and in ref.<sup>45</sup> do not present anomalous band shapes. This was demonstrated in ref.<sup>45</sup> by showing that the adsorption of a test molecule (carbon monoxide) leads to SEIRAS spectra with normal band-shape.

Further inspection of the spectra in Figure 3 reveals other interesting information. Since in these spectra the positive bands due to water molecules coadsorbed with perchlorate anions are absent, it is possible to study the negative bands in more detail. As above mentioned, these negative bands are due to water molecules adsorbed with their hydrogen atoms closer to the gold surface, and to hydronium-water complexes. It is observed that the intensity of these bands monotonously increases with potential, which suggests a monotonous decrease in the coverage of these species. These results strongly suggest that the adsorption of perchlorate anions does not involve the coadsorption of hydronium cations. Similar conclusions were previously obtained in relation to sulfate anions.<sup>45</sup>

Finally, we will discuss how to separate the positive and negative bands that are overlapping in the spectra in Figure 2. To perform such a separation, previous works used a reference spectrum located at intermediate potentials.<sup>28-30</sup> However, this strategy does not produce an accurate separation of the bands. This is illustrated in Figure 5, where the SEIRAS spectra in Figure 2 are plotted by using the spectrum at  $E=0.6\text{V}$  as the reference. It is observed that the cancellation of the negative bands in the spectra is not complete. These negative bands are due to species adsorbed at the reference potential. For the present system, any value of reference potential would lead to the appearance of negative adsorption bands.

Alternatively, the spectra in Figure 3 can be used to separate the positive and negative bands in the spectra in Figure 2. This is based on the fact that the bands associated to water molecules coordinating perchlorate anions are absent in the spectra in Figure 3. Thus, subtraction of the absorption bands in the spectra in Figure 3 from the spectra in Figure 2 should show the signatures of water coordinating perchlorate anions. The results are shown in Figure 6. These spectra exhibit the presence of a narrow  $\nu(\text{O-H})$  positive band at  $3610\text{ cm}^{-1}$ , a broader  $\nu(\text{O-H})$  positive band centered at  $3430\text{ cm}^{-1}$  and a

$\delta(\text{H-O-H})$  positive band at  $1650\text{ cm}^{-1}$ . It is clearly observed that the subtraction of the negative water signatures is accurate. Thus, the spectra in Figure 6 show that the bands associated with water coordinating perchlorate anions start to grow at  $E > 0.4\text{ V}$ , in harmony with the appearance of the  $\nu(\text{Cl-O})$  band of adsorbed perchlorate in Figures 2 and 3. It is apparent that the intensity of these bands is correlated with the intensity of the  $\nu(\text{Cl-O})$  band of adsorbed perchlorate, suggesting that these water molecules belong to the hydration shell of adsorbed perchlorate anions. In the spectra in Figure 6, it is also observed that the  $\nu(\text{Cl-O})$  band becomes bipolar. The origin of this bipolar band is not clear, and it could be an artifact associated to the subtraction procedure used here.

### 3.3. SEIRAS measurements in sulfuric acid solutions

At this point, it is interesting to reconsider the SEIRAS measurements in sulfuric acid solutions reported previously.<sup>45</sup> In view of the discussion of the results in perchloric acid solutions, we conclude that it is possible to separate the vibrational signatures of water coordinating to anions, from other contributions in the experimental SEIRAS spectra, by calculating the difference in the spectra measured with gold films prepared at different gold deposition rates. Therefore, it is interesting to perform such a calculation with the SEIRAS results in sulfuric acid solutions as well. The results are shown in Figure 7. Several similarities with respect to the corresponding difference spectra in  $0.1\text{ M HClO}_4$  in Figure 6 are observed:

-A positive  $\nu(\text{O-H})$  band grows at  $E > 0.4\text{ V}$ , similar to the behavior observed in perchloric acid solutions. However, in sulfuric acid solutions, there is a single band centered at  $3490\text{ cm}^{-1}$ , and its intensity increases much more markedly with potential than in perchloric acid solutions.

-Simultaneously, a positive  $\delta(\text{H-O-H})$  band appears at  $E > 0.4\text{ V}$ . This band is essentially the same as that found in perchloric acid solutions.

-Finally, a positive band associated with the S-O stretching,  $\nu(\text{S-O})$ , of adsorbed sulfate anions is also observed. The presence of this band in the difference spectra in Figure 7 is due to the fact that the intensity of this band increases if the gold films are made at an slower deposition rate.<sup>45</sup>

The bands due to water coordinating sulfate anions grow with increasing the applied potential in a way that parallels the increase in the intensity of the  $\nu(\text{S-O})$  band of adsorbed sulfate. Hence, these water bands likely belong to the hydration shell of coadsorbed sulfate anions.

The frequency of the  $\nu(\text{O-H})$  band of water coordinating to sulfate and perchlorate anions supports this explanation. Water molecules bonding to coadsorbed sulfate have a  $\nu(\text{O-H})$  frequency relatively close to bulk water, resembling water molecules in the hydration shell of sulfate anions in solution.<sup>25,26</sup> On the contrary, water molecules bonding to coadsorbed perchlorate show a blue-shifted  $\nu(\text{O-H})$  band, similar to the hydration shell of perchlorate anions in solution.<sup>25,26</sup>

Finally, it is also noteworthy that the comparison of Figures 6 and 7 clearly shows that the intensity of the  $\nu(\text{O-H})$  band of water molecules coordinating to sulfate anions is clearly higher than that with perchlorate anions. This is probably related to the larger strength of the hydrogen bond formed between sulfate anions and water molecules,<sup>46</sup> which can lead to a larger net orientation of the water molecules and a larger infrared absorption cross-section.

#### **4. Conclusions**

We have reported on the properties of water adsorption on gold from perchloric acid and sulfuric acid solutions, as a function of the applied potential, as studied by SEIRAS. It is observed that the structure of the gold films has a major impact on the adsorption of water. Gold films deposited at  $0.1 \text{ \AA/s}$  are mainly composed of nanoparticles of  $47 \pm 11 \text{ nm}$ , and the SEIRAS spectra measured with these films are in good agreement with previous works.<sup>28-30</sup> When the gold films are made at  $1 \text{ \AA/s}$ , the nanoparticle size is decreased to  $27 \pm 8 \text{ nm}$ . The SEIRAS spectra measured with those films show the characteristic bands due to water adsorbed with their hydrogen atoms closer to the metal at low potentials, and ice-like structured water at intermediate potentials, as is the case for gold films composed of larger nanoparticles. However, the SEIRAS bands associated with water molecules coordinating to coadsorbed anions are

absent, suggesting that the orientation of these water molecules is parallel with respect to the surface.

Finally, the combination of both types of measurements allows a more detailed study of the properties of water bonding to coadsorbed anions. This is done by subtracting the spectra measured with gold films made at 1 Å/s from the corresponding spectra measured at the same potential with gold films made at 0.1 Å/s. It is shown that the intensity of the SEIRAS bands of these water molecules increases with potential in a way that parallels the behavior of the  $\nu(\text{Cl-O})$  and  $\nu(\text{S-O})$  bands of coadsorbed perchlorate and sulfate anions, respectively. This indicates that these water molecules belong to the hydration shell of the coadsorbed anions. This notion is further supported by the observation that their  $\nu(\text{O-H})$  frequencies resemble those of water molecules in the hydration shells of these anions in bulk solution.<sup>25,26</sup>

## Acknowledgements

We would like to thank Prof. M. Osawa for pointing out the effect of the nanoparticle size on the spatial extent of the SEIRAS effect. We also gratefully acknowledge H. Zeijlemaker and H. Schoenmaker for their outstanding technical support. N.G.A. acknowledges the European Commission (FP7) for the award of a Marie Curie fellowship. P. M.K. and P.R. acknowledge financial support from the Netherlands organization for Scientific Research (NWO) through a VICI and a VENI grants.

## References:

- (1) Zope, B. N.; Hibbitts, D. D.; Neurock, M.; Davis, R. J. *Science* **2010**, *330*, 74-78.
- (2) Date, M.; Okumura, M.; Tsubota, S.; Haruta, M. *Angew.Chem.Int.Ed.* **2004**, *43*, 2129-2132.
- (3) *Fuel Cell Catalysis: A Surface Science Approach*. Ed.: Koper, M. T. M. John Wiley and Sons, Inc. Hoboken, New Jersey (USA), 2009.
- (4) Stamenkovic, V. R.; Fowler, B.; Mun, B. S.; Wang, G. F.; Ross, P. N.; Lucas, C. A.; Markovic, N. M. *Science* **2007**, *315*, 493-497.

- (5) Stamenkovic, V.; Mun, B. S.; Mayrhofer, K. J. J.; Ross, P. N.; Markovic, N. M.; Rossmeisl, J.; Greeley, J.; Norskov, J. K. *Angew.Chem.Int.Ed.* **2006**, *45*, 2897-2901.
- (6) Zhang, J.; Sasaki, K.; Sutter, E.; Adzic, R. R. *Science* **2007**, *315*, 220-222.
- (7) Thiel, P. A.; Madey, T. E. *Surf.Sci.Rep.* **1987**, *7*, 211-385.
- (8) Henderson, M. A. *Surf.Sci.Rep.* **2002**, *46*, 1-308.
- (9) Feibelman, P. J. *Science* **2002**, *295*, 99.
- (10) Ogasawara, H.; Brena, B.; Nordlund, D.; Nyberg, M.; Pelmenchikov, A.; Pettersson, L. G. M.; Nilsson, A. *Phys. Rev. Lett.* **2002**, *89*, 276102.
- (11) Vassilev, P.; van Santen, R. A.; Koper, M. T. M. *J.Chem.Phys.* **2005**, *122*, 054701.
- (12) Ito, M. *Surf.Sci.Rep.* **2008**, *63*, 329-389.
- (13) Santen, R. A. van; Neurock, M.; Shetty, S. G. *Chem.Rev.* **2010**, *110*, 2005.
- (14) Niet, M. J. T. C. van der; Dunnen, A. den; Juurlink, L. B. F.; Koper, M. T. M. *Angew.Chem.Int.Ed.* **2010**, *49*, 6572-6575.
- (15) Jiang, Y. X.; Li, J. F.; Wu, D. Y.; Yang, Z. L.; Ren, B.; Hu, J. W.; Chow, Y. L.; Tian, Z. Q. *Chem.Commun.* **2007**, 4608-4610.
- (16) Chen, T. T.; Owen, J. F.; Chang, R. K.; Laube, B. L. *Chem.Phys.Lett.* **1982**, *89*, 356-361.
- (17) Pettinger, B.; Philpott, M. R.; Gordon, J. G. *J.Chem.Phys.* **1981**, *74*, 934-940.
- (18) Fleischmann, M.; Hendra, P. J.; Hill, I. R.; Pemble, M. E. *J.Electroanal.Chem.* **1981**, *117*, 243-255.
- (19) Noguchi, H.; Okada, T.; Uosaki, K. *Faraday Discuss.* **2008**, *140*, 125-137.
- (20) Nihonyanagi, S.; Ye, S.; Uosaki, K.; Dreesen, L.; Humbert, Ch.; Thiry, P.; Peremans, A. *Surf.Sci.* **2004**, *573*, 11-16.
- (21) Schultz, Z. D.; Shaw, S. K.; Gewirth, A. A. *J.Am.Chem.Soc.* **2005**, *127*, 15916-15922.
- (22) Climent, V.; Coles, B. A.; Compton, R. G. *J.Phys.Chem.B* **2002**, *106*, 5988-5996.
- (23) Climent, V.; Coles, B. A.; Compton, R. G. *J.Phys.Chem.B* **2002**, *106*, 5258-5265.
- (24) Nagai, T.; Nakanishi, S.; Nakato, Y. *ChemPhysChem* **2007**, *8*, 1016-1018.

- (25) Ohtaki, H.; Radnai, T. *Chem.Rev.* **1993**, *93*, 1157-1204.
- (26) Bakker, H. J. *Chem.Rev.* **2008**, *108*, 1456-1473.
- (27) Bakker, H. J.; Skinner, J. L. *Chem.Rev.* **2010**, *110*, 1498-1517.
- (28) Ataka, K.; Yotsuyanagi, T.; Osawa, M. *J.Phys.Chem.* **1996**, *100*, 10664-10672.
- (29) Ataka, K. I.; Osawa, M. *Langmuir* **1998**, *14*, 951-959.
- (30) Wandlowski, T.; Ataka, K.; Pronkin, S.; Diesing, D. *Electrochim.Acta* **2004**, *49*, 1233-1247.
- (31) Cai, W.-B.; Wan, L.-J.; Noda, H.; Hibino, Y.; Ataka, K.; Osawa, M. *Langmuir* **1998**, *14*, 6992-6998.
- (32) Noda, H.; Ataka, K.; Wan, L.-J.; Osawa, M. *Surf.Sci.* **1999**, *427-428*; *1 June 1999*, 190-194.
- (33) Noda, H.; Minoha, T.; Wan, L. J.; Osawa, M. *J.Electroanal.Chem.* **2000**, *481*, 62-68.
- (34) Cai, W.-B.; Amano, T.; Osawa, M. *J.Electroanal.Chem.* **2001**, *500*, 147-155.
- (35) Noda, H.; Wan, L. J.; Osawa, M. *Phys.Chem.Chem.Phys.* **2001**, *3*, 3336-3342.
- (36) Futamata, M. *Surf.Sci.* **1999**, *427-428*, 179-183.
- (37) Futamata, M. *Chem.Phys.Lett.* **2000**, *317*, 304-309.
- (38) Futamata, M. *J.Phys.Chem.B* **2001**, *105*, 6933-6942.
- (39) Futamata, M. *J.Electroanal.Chem.* **2003**, *550-551*, 93-103.
- (40) Berna, A.; Delgado, J. M.; Orts, J. M.; Rodes, A.; Feliu, J. M. *Langmuir* **2006**, *22*, 7192-7202.
- (41) Delgado, J. M.; Berna, A.; Orts, J. M.; Rodes, A.; Feliu, J. M. *J. Phys. Chem. C* **2007**, *111*, 9943-9952.
- (42) Berna, A.; Delgado, J. M.; Orts, J. M.; Rodes, A.; Feliu, J. M. *Electrochim.Acta* **2008**, *53*, 2309-2321.
- (43) Delgado, J. M.; Blanco, R.; Orts, J. M.; Perez, J. M.; Rodes, A. *J. Phys. Chem. C* **2009**, *113*, 989-1000.
- (44) Hasegawa, T.; Nishijo, J.; Imae, T.; Huo, Q.; Leblanc, R. M. *J.Phys.Chem.B* **2001**, *105*, 12056-12060.

- (45) Garcia-Araez, N.; Rodriguez, P.; Navarro, V.; Bakker, H. J.; Koper, M. T. M. *J. Phys. Chem. C* **2011**, *115*, 21249.
- (46) Tielrooij, K. J.; Garcia-Araez, N.; Bonn, M.; Bakker, H. J. *Science* **2011**, *328*, 1006-1009.
- (47) Hamelin, A. *J. Electroanal. Chem.* **1986**, *210*, 303-9.
- (48) Sun, S.-G.; Cai, W.-B.; Wan, L.-J.; Osawa, M. *J. Phys. Chem. B* **1999**, *103*, 2460-2466.
- (49) Akiyama, R.; Hirata, F. *J. Chem. Phys.* **1998**, *108*, 4904-4910.
- (50) Duan, S.; Wu, D. Y.; Xu, X.; Luo, Y.; Tian, Z. Q. *J. Phys. Chem. C* **2010**, *114*, 4051-4056.
- (51) Sadkowski, A.; Motheo, A. J.; Neves, R. S. *J. Electroanal. Chem.* **1998**, *455*, 107-119.
- (52) Chen, N.; Blowers, P.; Masel, R. I. *Surf. Sci.* **1999**, *419*, 150-157.
- (53) Simeone, F. C.; Kolb, D. M.; Venkatachalam, S.; Jacob, T. *Surf. Sci.* **2008**, *602*, 1401-1407.
- (54) Meng, S.; Wang E.G.; Gao, S. *Phys. Rev. B* **2004**, *69*, 195404.
- (55) Chang, C. I.; Lee, W. J.; Young, T. F.; Ju, S. P.; Chang, C. W.; Chen, H. L.; Chang, J. G. *J. Chem. Phys.* **2008**, *128*, 154703.
- (56) Park, S.; Odelius, M.; Gaffney, K. J. *J. Phys. Chem. B* **2009**, *113*, 7825-7835.
- (57) Walrafen, G. E. *J. Chem. Phys.* **2005**, *122*, 094510.
- (58) Osawa, M. *Near-Field Optics and Surface Plasmon Polaritons. Topics in Applied Physics, vol. 81.* Ed.: Kawata, S. Springer. **2001**, p.163-187.
- (59) Pettinger, B.; Domke, K.; Zhang, D.; Schuster, R.; Ertl, G. *Phys. Rev. B* **2007**, *76*, 113409.
- (60) Pettinger, B.; Domke, K.; Zhang, D.; Picardi, G.; Schuster, R. *Surf. Sci.* **2009**, *603*, 1335-1341.
- (61) Dretschkow, T.; Wandlowski, T. *Ber. Bunsen-Ges.* **1997**, *101*, 749-757.
- (62) Michaelides, A.; Ranea, V. A.; de Andres, P. L.; King, D. A. *Phys. Rev. Lett.* **2003**, *90*, 216102.

## Figures Captions

Figure 1. Steady-state cyclic voltammogram of a thin gold film of 20 nm in 0.1 M HClO<sub>4</sub>. Scan rate= 50 mV/s.

Figure 2. SEIRAS spectra at different potentials measured with a gold thin film of 20 nm, deposited at 0.1 Å/s, and put in contact with a solution of 0.1M HClO<sub>4</sub>. The reference spectrum was taken at  $E_{\text{ref}}=0.05$  V.

Figure 3. As in Figure 2, but with the thin gold film deposited at 1 Å/s.

Figure 4. Proposed model structures of water molecules adsorbed on gold.

Figure 5. The same spectra as in Figure 2, but using the spectrum measured at  $E_{\text{ref}}=0.6$  V as the reference spectrum.

Figure 6. Difference spectra obtained by subtracting the spectra of Figure 3 from those of Figure 2.

Figure 7. SEIRAS spectra of a gold film in contact with a solution of 0.1 M H<sub>2</sub>SO<sub>4</sub>. The spectra shown are difference spectra and are obtained by subtracting the spectra measured for a gold film deposited at 1 Å/s from the spectra measured for a gold film deposited at 0.1 Å/s.

## Figures

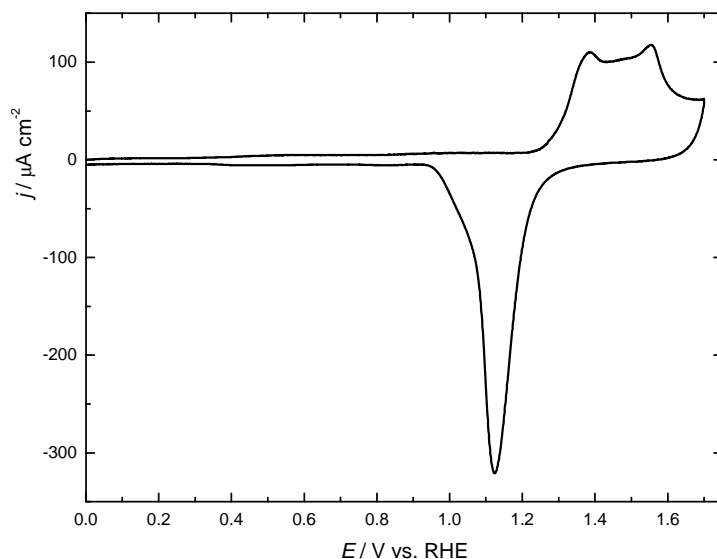


Figure 1. Steady-state cyclic voltammogram of a thin gold film of 20 nm in 0.1 M HClO<sub>4</sub>. Scan rate= 50 mV/s.

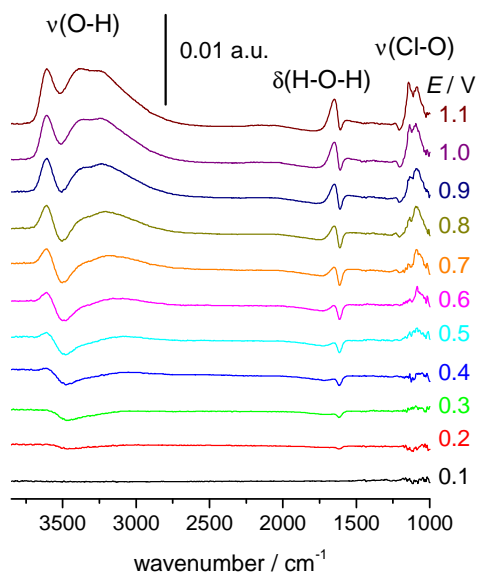


Figure 2. SEIRAS spectra at different potentials measured with a gold thin film of 20 nm, deposited at 0.1 Å/s, and put in contact with a solution of 0.1M HClO<sub>4</sub>. The reference spectrum was taken at  $E_{\text{ref}}=0.05$  V.

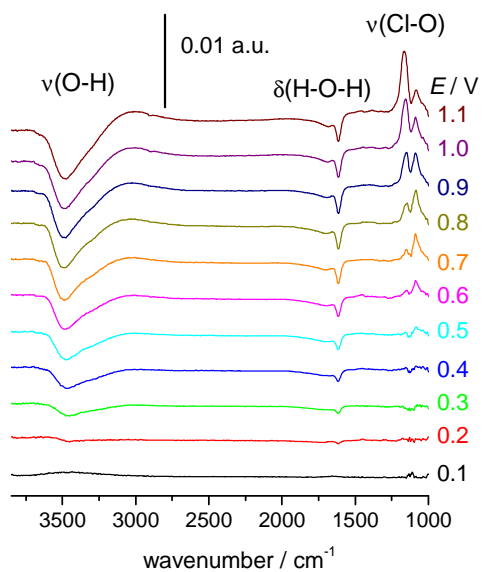


Figure 3. As in Figure 2, but with the thin gold film deposited at 1 Å/s.

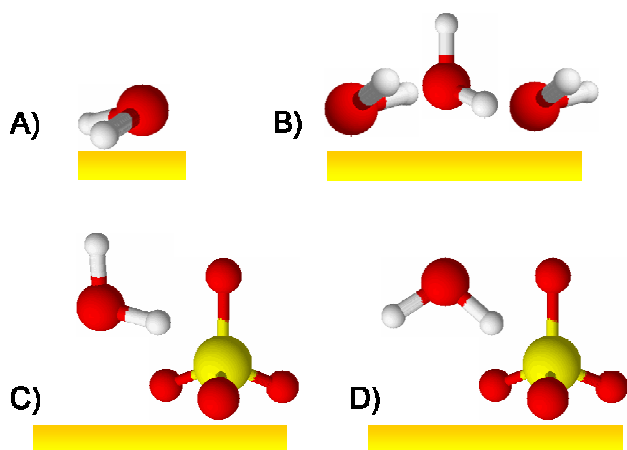


Figure 4. Proposed model structures of water molecules adsorbed on gold.

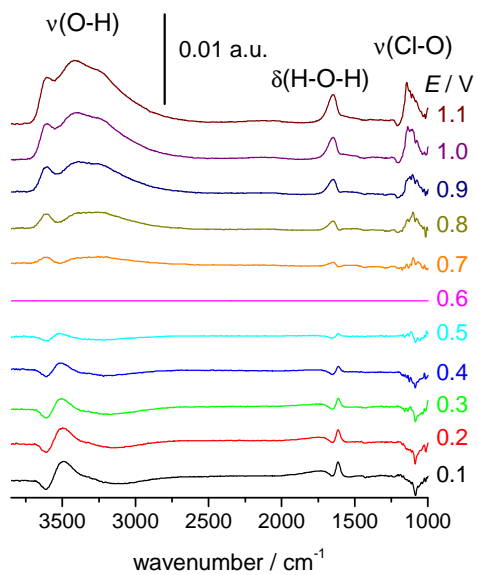


Figure 5. The same spectra as in Figure 2, but using the spectrum measured at  $E_{\text{ref}}=0.6$  V as the reference spectrum.

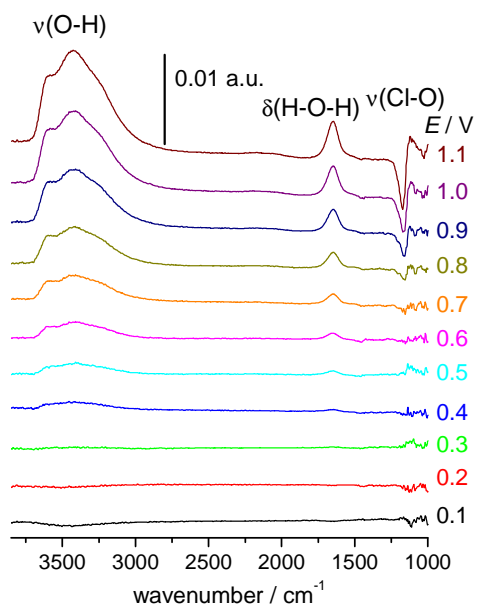


Figure 6. Difference spectra obtained by subtracting the spectra of Figure 3 from those of Figure 2.

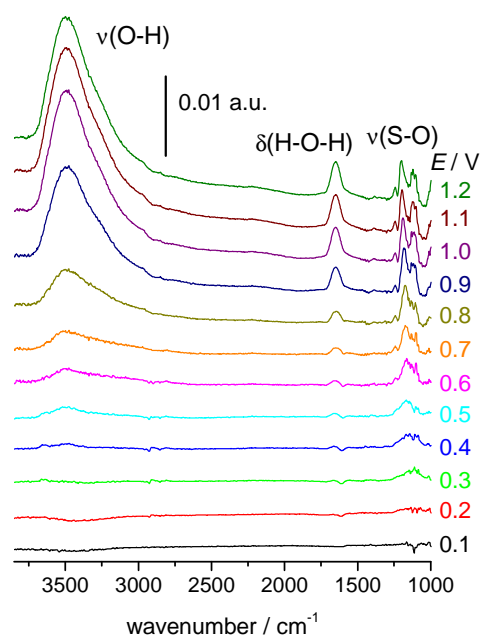


Figure 7. SEIRAS spectra of a gold film in contact with a solution of 0.1 M H<sub>2</sub>SO<sub>4</sub>. The spectra shown are difference spectra and are obtained by subtracting the spectra measured for a gold film deposited at 1 Å/s from the spectra measured for a gold film deposited at 0.1 Å/s.

TOC graphic

